DOI: 10.1002/ejic.201001144

Crystal Structures and Conductivities of Two Organic–Inorganic Hybrid Complexes Based on Poly-Keggin-Anion Chains

Mei-Lin Wei,*[a] Peng-Fei Zhuang,[a] Hui-Hua Li,[a] and Yun-Hui Yang[a]

Keywords: Organic-inorganic hybrid composites / Conducting materials / Polyoxometalates / Structure elucidation

Two proton-conducting organic–inorganic hybrid complexes have been constructed by the self-assembly of protonated water clusters, transition-metal aqua ions, $[PMo_{12}O_{40}]^{3-}$ anions and isonicotinic acid *N*-oxide (HINO). Single-crystal X-ray diffraction analyses at 293 K revealed that both complexes presented exactly the same three-dimensional supramolecular framework built from non-covalent interactions. Interestingly, the $[PMo_{12}O_{40}]^{3-}$ anions self-assembled into poly-Keggin-anion chains in the supramolecular frameworks. Thermogravimetric analyses showed no weight loss for either system in the temperature range of 20–100 °C, which indicates that none of the water molecules in the unit structure are easily lost below 100 °C. Surprisingly, the proton conductivities of **1** and **2** in the temperature range of 85–100 °C under 98 % relative humidity reached good proton conductivities of 10^{-3} S cm^{-1}. A possible mechanism for the proton conduction in accord with experimental results is proposed.

Introduction

Keggin-type heteropoly acids (HPAs) possessing a unique discrete ionic structure, including heteropoly anions and countercations (H^+, H_3O^+, $H_5O_2^+$, etc.), are widely known as proton-conducting electrolytes for low-temperature hydrogen/oxygen fuel cells.[1] However, the application of HPAs is limited by the extreme sensitivity of their conductivity to the relative humidity (RH) and temperature of the surrounding atmosphere.[2] To overcome these problems, various attempts have been made to immobilize HPAs in silica gel and to disperse this into an organically modified electrolyte membrane and organic–inorganic hybrid membranes.[3,4] In addition, to enable fast ionic conduction in the hybrid materials, the molecular modification of organic ligands to inorganic structures of HPAs has been continuously investigated.[5] However, so far, there has been no report of highly proton-conducting hybrid materials based on transition-metal salts of HPAs. For a long time we focused on the proton conductivity of organic–inorganic complexes based on the transition-metal salts of HPAs dispersed in self-ordered hydrogen-bonded networks. Salts crystallize with fewer water molecules than the acids and are more stable. The incorporation of salts into self-ordered hydrogen-bonded networks protects them from dehydration and enhances their thermal stability. Moreover, each transition-metal ion could form an ionized water cluster with a special hydration number and a special structure. In the work reported herein, we succeeded in constructing two proton-conducting organic–inorganic hybrid complexes by the self-assembly of protonated water clusters, transition-metal aqua ions, $[PMo_{12}O_{40}]^{3-}$ anions and isonicotinic acid *N*-oxide (HINO). Herein, we report their syntheses, crystal structures and proton conductivities as a function of temperature.

Results and Discussion

Complexes **1** and **2**, $\{[M(H_2O)_8][H(H_2O)_{2.5}](HINO)_4(PMo_{12}O_{40})\}_n$ (M = Co for **1**, M = Ni for **2**), were synthesized by the reaction of $MHPMo_{12}O_{40}{\cdot}nH_2O$ and HINO at room temperature. They were characterized by single-crystal X-ray diffraction, infrared spectroscopy, TG and elemental analyses. X-ray diffraction analyses at 293 K revealed that both complexes crystallized in the orthorhombic space group *Pnnm*, exhibited very similar unit cell parameters and presented exactly the same 3D supramolecular frameworks built from non-covalent interactions between HINO molecules, $[M(H_2O)_8]^{2+}$ and $H^+(H_2O)_{2.5}$ clusters and $[PMo_{12}O_{40}]^{3-}$ anions. Interestingly, $[PMo_{12}O_{40}]^{3-}$ anions self-assembled into poly-Keggin-anion chains in supramolecular frameworks. For a clear structural description of both compounds, the same labelling was used.

In the $[M(H_2O)_8]^{2+}$ aqua complex (Figure 1, a), the M^{2+} ion is placed at the symmetry centre and located in an octahedral coordination environment constructed of six water molecules [two O(1W) centres, two O(2W) centres and two O(3W) centres] with two O(4W) centres dangling outside

[a] College of Chemistry and Environmental Science,
Henan Normal University,
46# East of Construction Road, Xinxiang 453007, P. R. China
Fax: +86-373-3329281
E-mail: weimeilinhd@163.com

Supporting information for this article is available on the WWW under http://dx.doi.org/10.1002/ejic.201001144.

of the coordination shell through short hydrogen-bonding interactions with the coordination water molecule. Note that two O(3W) centres are crystallographically disordered into four symmetrical positions with each oxygen site half-occupied and that two O(2W) centres are also crystallographically disordered into four symmetrical positions with each oxygen site half-occupied. In the $H^+(H_2O)_{2.5}$ unit (the proton added to balance the charge)[6] (Figure 1, b), the O(5W) atom with an occupancy of 50% is placed in a symmetry centre and located in a tetragonal environment built from two water molecules [O(6W) and O(7W) centres], which are crystallographically disordered into two symmetrical positions with each oxygen site half-occupied, respectively. The hydrogen-bonding distance between O(6W) and O(7W) is 2.676(17) Å for **1** and 2.626 Å for **2**. The existence of these half-occupied oxygen sites of water molecules in $[M(H_2O)_8]^{2+}$ and $H^+(H_2O)_{2.5}$ clusters may be conducive to the formation of a hydrogen-bonding network and to proton transport along the hydrogen-bonding network.[7]

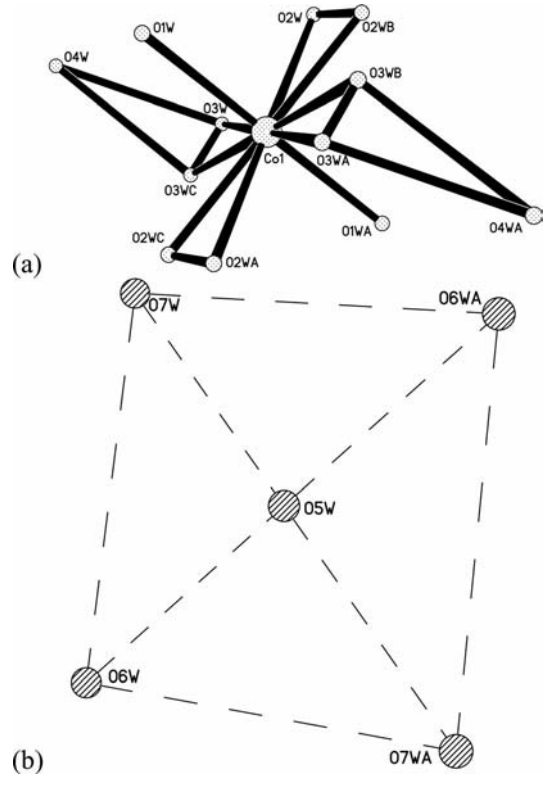

Figure 1. View of (a) the $[M(H_2O)_8]^{2+}$ and (b) the $H^+(H_2O)_{2.5}$ clusters. Hydrogen atoms have been omitted for clarity. Selected bond lengths [Å] for complex **1**: Co(1)–O(1W) 2.105(7), Co(1)–O(2W) 2.035(9), Co(1)–O(3W) 2.095(10), O(4W)···O(3W) 2.59(2); for complex **2**: Ni(1)–O(1W) 2.046(9), Ni(1)–O(2W) 1.989(10), Ni(1)–O(3W) 2.057(14), O(4W)···O(3W) 2.60(2).

Interestingly, HINO molecules are not bound to the M^{2+} ion, but remain outside of the coordination shell to form hydrogen-bonded chains along the *b* axis (Figure 2). Two oxygen atoms, O(15) (N–O) and O(17) (O–H), of each HINO molecule are involved in the hydrogen-bonded chains. As shown in Figure 3, these HINO hydrogen-bonded chains are linked together by $[M(H_2O)_8]^{2+}$ aqua complexes and small $H^+(H_2O)_{2.5}$ clusters into a 3D cationic network with large 1D channels through hydrogen bonds between coordination water molecules O(2W) and oxygen atoms O(15) of the HINO molecules, between water molecules O(6W) and oxygen atoms O(15) of the HINO molecules as well as through weak hydrogen bonds between coordination water molecules and oxygen atoms of the HINO molecules. Thus, all the O atoms of each HINO molecule are involved in hydrogen bonds, creating a 3D supramolecular assembly with 1D channels. Moreover, there are hydrogen-bonding interactions between water molecules O(7W) in the $H^+(H_2O)_{2.5}$ clusters and O(1W) centres of the $[M(H_2O)_8]^{2+}$ cluster. The section size of the channels based on the M···M separations is around $10.3 \times 16.0 \times 19.8$ Å for **1** and $10.2 \times 15.9 \times 19.7$ Å for **2** (these separations are equal to three axial lengths, respectively), which indicates that each pore could only accommodate a single Keggin anion. Interestingly, the M···M separation bridged by the $H^+(H_2O)_{2.5}$ clusters along the *a* axis is much shorter than the other two separations along the *b* and *c* axes, and even shorter than the diameter of the discrete $[PMo_{12}O_{40}]^{3-}$ anion (ca. 10.4 Å), which results in each cavity being heavily condensed along the *a* axis. In addition, the presence of positively charged species, $[M(H_2O)_8]^{2+}$ and $H^+(H_2O)_{2.5}$ clusters, could attract the polyanions and as a result the Keggin-type $[PMo_{12}O_{40}]^{3-}$ anions for charge compensation are embedded in the voids of the 3D cationic framework

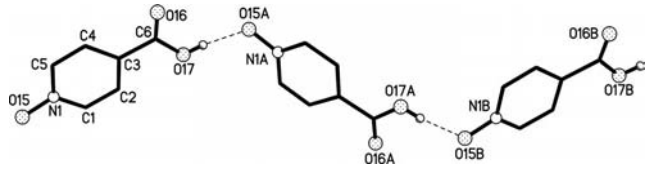

Figure 2. View of the 1D HINO chain along the *b* axis. Hydrogen atoms have been omitted for clarity. Selected atom···atom distances [Å] for complex **1**: O(17)···O(15A) 2.62(2); for complex **2**: O(17)···O(15A) 2.59(2). Symmetry code, A: $-x + {}^5/_2$, $y - ½$, $-z + ½$.

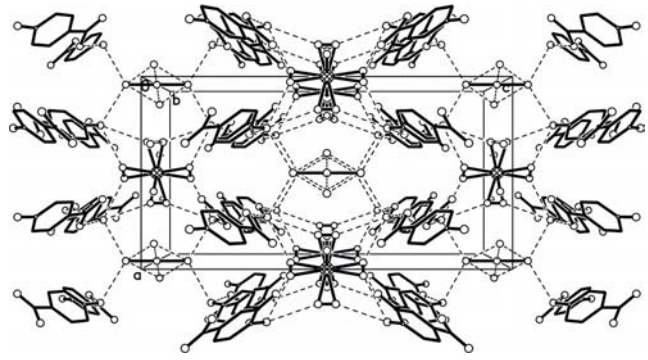

Figure 3. Representative 3D hydrogen-bonded network constructed of HINO molecules, $[M(H_2O)_8]^{2+}$ and $H^+(H_2O)_{2.5}$ clusters. Hydrogen atoms have been omitted for clarity. Selected atom···atom distances [Å] for complex **1**: O(1W)···O(16A) 3.016(2), O(2W)···O(16A) 2.948(2), O(3W)···O(15B) 2.928(2), O(7W)···O(1W) 2.979(3); for complex **2**: O(1W)···O(16A) 2.940(2), O(2W)···O(16A) 2.955(3), O(3W)···O(15B) 2.914(2), O(7W)···O(1W) 2.983(3). Symmetry code, A: $-x + {}^3/_2$, $y + ½$, $-z + ½$; B: $-x + 1$, $-y - 1$, $-z$.

and connect to one another leading to poly-Keggin-anion chains in the channel along the *a* axis (Figure 4). In the polymeric polyanion, there are some short atom···atom separations of 2.99(2) Å, for example, O(7A)···O(8BB), O(8A)···O(7BB), O(7AA)···O(8CB) and O(7CB)···O(8AA).

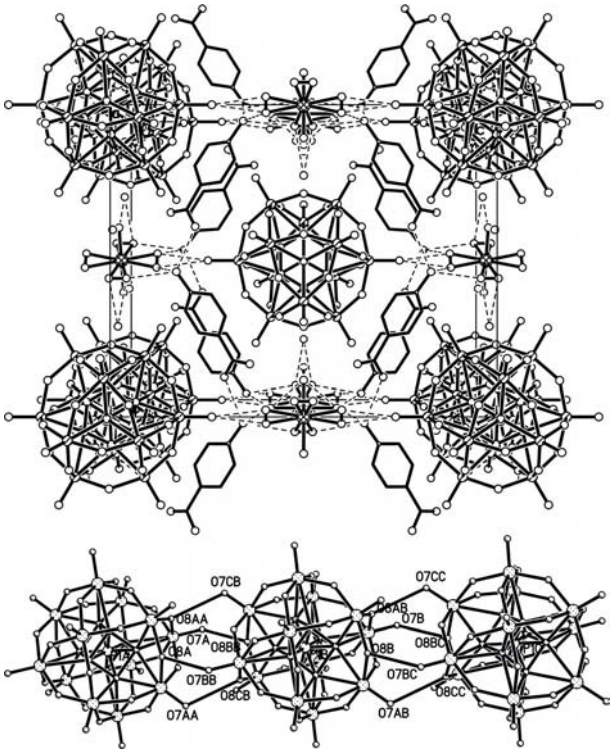

Figure 4. Representative 3D hydrogen-bonded network showing $[PMo_{12}O_{40}]^{3-}$ anions self-assembled into poly-Keggin-anion chains in asupramolecular framework along the *a* axis (top) and view of the poly-anion chain along the *a* axis (bottom). Hydrogen atoms have been omitted for clarity. Selected atom···atom distances [Å] for complex **1**: O(2W)···O(12A) 2.793(2), O(4W)···O(9) 2.918(2), O(7W)···O(11) 3.130(3); for complex **2**: O(2W)···O(12A) 2.796(2), O(4W)···O(9) 2.921(2), O(7W)···O(11) 3.134(3). Symmetry code, A: $-x + {}^3/_2$, $y + ½$, $-z + ½$.

In the $[PMo_{12}O_{40}]^{3-}$ unit, the central P atom is surrounded by a cube of eight oxygen atoms with each oxygen site half-occupied. These eight oxygen atoms are all crystallographically disordered and this case can be found in many compounds.[6] In complex **1**, the bond lengths of P–O and Mo–O are 1.509(10)–1.536(7) and 1.649(6)–2.488(8) Å, respectively. In complex **2**, the bond lengths of P–O and Mo–O are 1.515(12)–1.525(8) and 1.641(5)–2.470(11) Å, respectively. The bond lengths of P–O and Mo–O in the two complexes are comparable to those in the 3D porous polyoxometallate-based organic–inorganic hybrid materials with Keggin anions as guests.[6] In addition, the O–P–O angles are in the range of 109.3(3)–109.9(5)° for **1** and 108.8(6)–109.7(4)° for **2**. All these results indicate that the $[PMo_{12}O_{40}]^{3-}$ units have a normal Keggin structure in the polymeric polyanion chains. The poly-Keggin-type anions play not only a charge-compensating role, but they can dramatically influence the overall solid-state architecture through their templating function, and the cationic framework with special channels also influences the polymerization of polyanions through its host function. In addition, several hydrogen bonds exist between the poly-Keggin-anion chain and the channel, for example, between the water molecules O(2W) and O(4W) of the $[M(H_2O)_8]^{2+}$ clusters and O(9) and O(12) centres of the polyanions as well as between water molecules O(7W) in the $H^+(H_2O)_{2.5}$ clusters and O(11) centres of the polyanions. As a result, based on the self-assembly of HINO molecules, $[M(H_2O)_8]^{2+}$ and $H^+(H_2O)_{2.5}$ clusters, both complexes form 3D hydrogen-bonding networks with 1D channels along the *a* axis in which poly-Keggin-anion chains are formed and stabilized by electrostatic and hydrogen-bonding interactions, resulting in $[PMo_{12}O_{40}]^{3-}$ anions not easily dissociated from the hybrid networks. Moreover, the section sizes of the channels along the *b* and *c* axes are so much larger than the diameter of the $[PMo_{12}O_{40}]^{3-}$ anion (ca. 10.4 Å) that there is enough space outside the poly-Keggin-anion chains to admit some small species, such as water molecules or hydronium ions, to transport along the channels. All these results indicate that **1** and **2** are potentially new, good proton-conducting materials.

These complexes are insoluble in water (see the UV spectral analyses in the Supporting Information). Water retention in the hybrid at a high temperature is a key factor for fast protonic conduction.[3,4] Thermogravimetric analyses of the powders of the crystalline samples of the two complexes under N_2 (Figure 5) show no weight loss in the temperature range of 20–100 °C, which indicates that all the

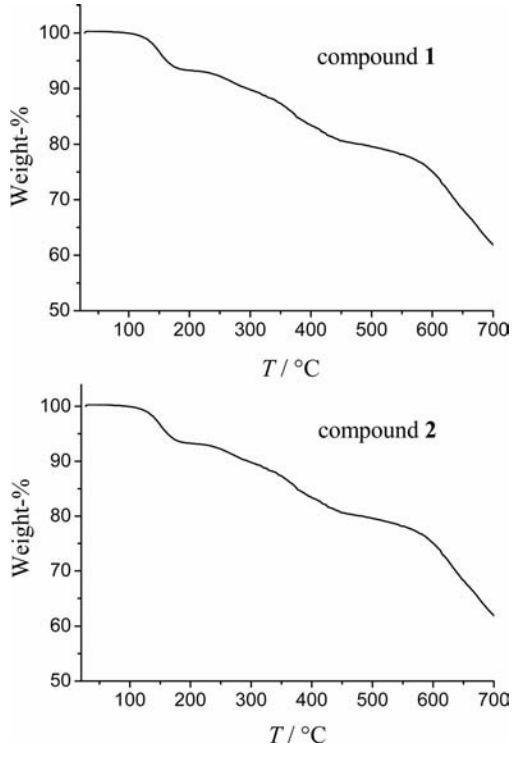

Figure 5. Perkin–Elmer thermogravimetric analyses of complexes **1** and **2** under N_2.

water molecules in the unit structure are involved in the construction of the hydrogen-bonding network, consistent with the results of the structural analysis, and are not easily lost below 100 °C. This is not the behaviour observed in proton conductors involving quasi-liquid water clusters (which are generally loosely bonded in the structure), such as the Nafion membrane[8,9] and pure tungstophosphoric acid (PWA-26) or molybdophosphoric acid (PMA-26), as well as many proton-conducting composite membranes doped with HPAs.[1,2] Interestingly, the global frameworks of the two complexes are retained when the water molecules are lost at 200 °C (see the powder X-ray diffraction analyses in the Supporting Information). All these results also indicate that **1** and **2** are potentially good proton-conducting materials.

The proton conductivities of **1** and **2** in the temperature range of 25–100 °C were therefore evaluated by the ac impedance method using a compacted pellet of the powdered crystalline sample. At 25 °C, both complexes showed poor proton conductivities of around 9.0×10^{-9} S cm^{-1} under 35% RH, estimated from the Nyquist plots shown in the Supporting Information, but their proton conductivities reached around 3.8×10^{-6} S cm^{-1} with a RH up to 98%. We also measured their ionic conductivities up to 100 °C under 98% RH. Surprisingly, both complexes showed good proton conductivities of $(1.42–2.83) \times 10^{-3}$ S cm^{-1} in the temperature range of 85–100 °C. These proton conductivities are about two orders of magnitude lower than that of a Nafion membrane, which shows conductivity of about 10^{-1} S cm^{-1} under the conditions described.[8,9]

Figure 6 shows the Arrhenius plots of the proton conductivities of the complexes in the temperature range of 25–100 °C under 98% RH. $\ln\sigma T$ increases almost linearly with temperature from 25 to 100 °C, and the corresponding activation energy (E_a) of conductivity was estimated to be 0.79 eV for **1** and 0.80 eV for **2** from Equation (1) in which σ is the ionic conductivity, σ_0 is the pre-exponential factor, k_B is the Boltzmann constant and T is the temperature. Both E_a values are very high. The results show that the general features of the changes in conductivities are different to those of a protonic conducting polymer membrane such as Nafion, which has almost identical protonic conductivity over a wide temperature range from ambient to 100 °C with an activation enthalpy of approximately 0.15 eV when it is fully humidified,[8,9] and are different to those of PWA-26 or PMA-26, whose protonic conductivity decreases with temperature from ambient to 60 °C.[1,2] However, the title complexes have thermally activated protonic conductivities[2d,7b] from 25 to 100 °C; as the temperature increases, the proton conductivities increase on a logarithmic scale even with almost saturated humidities. This is probably due to the fact that the protons belong to protonated water clusters and those originating from water molecules need a thermally activated process for dissociation as hydrated forms such as H^+, H_3O^+ or other proton species at a distance from $[PMo_{12}O_{40}]^{3-}$ clusters.[10]

$$\sigma T = \sigma_0 \exp(-E_a/k_B T) \quad (1)$$

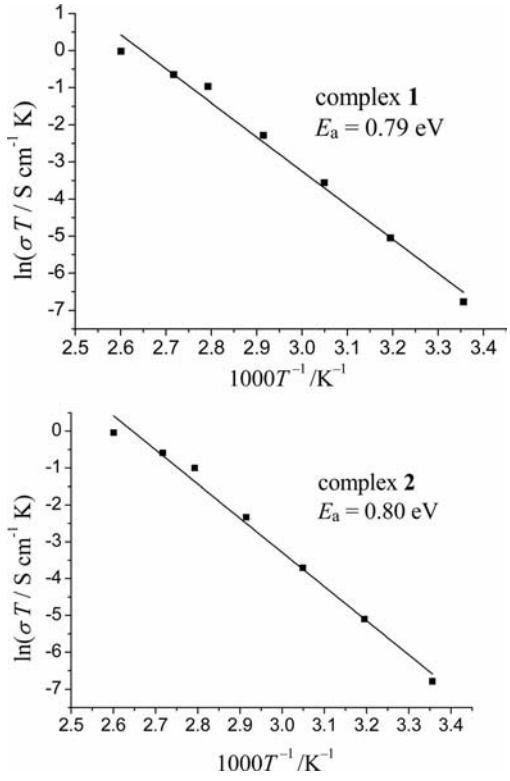

Figure 6. Arrhenius plots of the proton conductivities of complexes **1** and **2**.

The mechanism of proton conduction of **1** and **2** is, therefore, expected to be similar to that of the vehicle mechanism,[11] that is, the direct diffusion of additional protons with water molecules. In addition, the existence of hydrogen-bonding networks suggests that proton conduction in the two complexes includes some other process such as the proton transport of additional protons along hydrogen-bonding networks (Grotthus mechanism).[12] The fact that the two complexes exhibit good proton conductivities in the temperature range of 85–100 °C is indicative of a high carrier concentration based on a thermally activated process as well as the existence of hydrogen-bonding networks. Moreover, there is the possibility of hydrolysis of the complexes when they are held at 100 °C with a RH higher than 98% (100%, or condensed water that attacks the metal centres). The powder X-ray diffraction data in the Supporting Information suggest that the powder samples after the proton-conductive measurement have the same supramolecular frameworks as those of complexes **1** and **2**.

Interestingly, for complexes **1** and **2**, although the M^{2+} ion is different, they have the same 3D hydrogen-bonded networks and similar proton conductivities, which suggests that Co^{2+} and Ni^{2+} ions could form similar transition-metal aqua ions and that the origin of proton conduction in these complexes is based on the self-ordered hydrogen-bonding structures and the poly-Keggin-anion chains.

Conclusions

Two good proton-conducting organic/inorganic complexes have been constructed by introducing Keggin-type

polyanions as countercations and templates into the 3D cationic hydrogen-bonded networks formed by mixed ionized water clusters and HINO molecules. The organic–inorganic hybrid matrix changed the environment around the transition-metal salts of HPAs and influenced the formation of poly-Keggin anions within the resultant structure. Thus, the synthesis of these complexes provides a new route to increasing the stability and proton conductivity of organic–inorganic hybrid materials based on the salts of HPAs at high temperature, as well as the complexes themselves possibly being a new type of proton-conducting additive in proton-exchange composite membranes for use under dry and/or elevated temperature conditions in a fuel cell.

Experimental Section

General: All organic solvents and materials used for syntheses were of reagent grade and used without further purification. α-$H_3PMo_{12}O_{40}·6H_2O$ was prepared according to a literature method[13] and characterized by IR spectroscopy and TG analysis. HINO was synthesized according to a literature method and characterized by IR spectroscopy.[14] Elemental analyses (C, H and N) were performed with a Perkin–Elmer 240C analyser. IR spectra were recorded with a VECTOR 22 Bruker spectrophotometer with KBr pellets in the 400–4000 cm^{-1} region at room temperature. Thermogravimetric analyses were performed with a Perkin–Elmer thermal analyser under nitrogen at a heating rate of 10 °C min^{-1}. For the electrical conductivity study, the powdered crystalline samples were compressed to 0.7–1.0 mm in thickness and 12.0 mm in diameter under a pressure of 12–14 MPa. Alternating current (ac) impedance spectroscopy was performed with a chi660b (Shanghai chenhua) electrochemical impedance analyser with copper electrodes[15] (the purity of Cu was higher than 99.8%) over the frequency range of 10^5 to 10 Hz. Samples were placed in a temperature/humidity controlled chamber (GT-TH-64Z, Dongwan Gaotian Corp.) The conductivity was calculated from $\sigma = (1/R) \times (h/S)$ in which R is the resistance, h is the thickness and S is the area of the tablet.

Complex 1: The hereropolyacid cobalt salts were prepared by neutralization of the acid α-$H_3PMo_{12}O_{40}·6H_2O$ (120 mg, 0.06 mmol) and adding $CoCl_2·6H_2O$ (15 mg, 0.06 mmol) dissolved in water (4 mL). The solution was heated at 80 °C in a water bath. Yellow crystals were formed by cooling the saturated solution and allowing it to slowly evaporate at room temperature. They were characterized by IR spectroscopy. A mixture of the resulting heteropoly acid cobalt salts (60 mg, 0.03 mmol) and HINO (17 mg, 0.12 mmol) was dissolved in enough acetonitrile/water (1:1, v/v) solution. Finally, the solution was filtered and left to evaporate at room temperature. Red crystals appeared 4–5 d later and were collected and dried in air after quickly being washed with water; yield 51.6 mg, 86%, based on α-$H_3PMo_{12}O_{40}·6H_2O$. IR (KBr disk): four characteristic vibrations resulting from heteropoly anions with the Keggin structure: $\tilde{\nu}$: 803 ν(Mo–Oc), 878 ν(Mo–Ob), 961 ν(Mo=Ot), 1065 ν(P–Oa); and other vibrations resulting from the HINO molecules: 3326 ν(O–H), 1697 ν(C=O), 1618 ν(C=C), 1204 ν(N–O), 1168 δ(C–H, in plane) cm^{-1}. $C_{24}H_{42}CoMo_{12}N_4O_{62.5}P$ (2627.8): calcd. C 10.97, H 1.61, N 2.13; found C 10.91, H 1.64, N 2.17.

Complex 2: Complex **2** was prepared in the same way as **1**, except by using $NiCl_2·6H_2O$ (15 mg, 0.06 mmol) in place of $CoCl_2·6H_2O$; yield 51.0 mg, 85%, based on α-$H_3PMo_{12}O_{40}·6H_2O$. IR (KBr disk): four characteristic vibrations resulting from heteropoly anions with the Keggin structure: $\tilde{\nu}$ = 802 ν(Mo–Oc), 879 ν(Mo–Ob), 961 ν(Mo=Ot), 1064 ν(P–Oa); and other vibrations resulting from the HINO molecules: 3326 ν(O–H), 1696 ν(C=O), 1618 ν(C=C), 1203 ν(N–O), 1169 δ(C–H, in plane) cm^{-1}. $C_{24}H_{42}N_4O_{62.5}NiMo_{12}P$ (2627.58): calcd. C 10.97, H 1.61, N, 2.13; found C 10.90; H 1.64, N 2.19.

Crystal Structure Determination: Intensity data for complexes **1** and **2** were collected with a Siemens SMART-CCD diffractometer with graphite-monochromated Mo-K_α radiation (λ = 0.71073 Å) using the SMART and SAINT programs.[16] The structures were solved by direct methods and refined on F^2 by using full-matrix least-squares methods with SHELXTL.[17] For **1** and **2**, all non-hydrogen atoms except solvent water molecules were refined anisotropically. Hydrogen atoms of organic molecules were localized in their calculated positions and refined using a riding model. Hydrogen atoms of coordinated water molecules and solvent water molecules were not treated. The crystal parameters, data collection and refinement results for the two complexes are summarized in Table 1.

Table 1. Crystal data and structure refinement for complexes **1** and **2**.

	1	**2**
Chemical formula	$C_{24}H_{42}CoMo_{12}N_4O_{62.5}P$	$C_{24}H_{42}NiMo_{12}N_4O_{62.5}P$
Formula mass	2627.8	2627.58
Crystal system	orthorhombic	orthorhombic
Space group	*Pnnm*	*Pnnm*
a [Å]	10.2757(11)	10.204(6)
b [Å]	16.0203(17)	15.868(9)
c [Å]	19.855(2)	19.707(12)
a [°]	90.00	90.00
V [Å^3]	3268.6(6)	3191(3)
Z	2	2
Density [g cm^{-3}]	2.670	2.735
μ [mm^{-1}]	2.621	2.720
F(000)	2520	2522
T [K]	293(2)	293(2)
Independent reflections	2507	2181
R_{int}	0.0887	0.0827
Goodness-of-fit on F	0.948	1.092
$R1$ [$I>2\sigma(I)$]	0.0409	0.0433
$wR2$ [$I>2\sigma(I)$]	0.1282	0.1233

CCDC-795509 (for **1**) and -795510 (for **2**) contain the supplementary crystallographic data for this paper. These data can be obtained free of charge from The Cambridge Crystallographic Data Centre via www.ccdc.cam.ac.uk/data_request/cif.

Supporting Information (see footnote on the first page of this article): Crystal data of two complexes, the Nyquist plots for two complex**es** at 25–100 °C under 98% relative humidity, the UV spectra and the powder X-ray difraction data.

Acknowledgments

This work was supported by the National Natural Science Foundation of China (grant number 20971038) and the Natural Science Foundation of the Education Department of Henan Province (grant number 2009A150015).

[1] a) O. Nakamura, T. Kodama, I. Ogino, Y. Miyake, *Chem. Lett.* **1979**, 17–18; b) M. Misono, *Chem. Commun.* **2001**, 1141–1152; c) R. C. T. Slade, J. Barker, H. A. Pressman, J. H. Strange, *Solid State Ionics* **1988**, *28–30*, 594–600; d) D. E. Katsoulis, *Chem.*

Rev. **1998**, *98*, 359–287; e) J. L. Malers, M. A. Sweikart, J. L. Horan, J. A. Turner, A. H. Herring, *J. Power Sources* **2007**, *172*, 83; f) A. M. Herring, *Polym. Rev.* **2006**, *46*, 245.

[2] a) G. Alberti, M. Casciola, U. Costantino, A. Peraio, T. Rega, *J. Mater. Chem.* **1995**, *5*, 1809; b) G. Alberti, M. Casciola, *Solid State Ionics* **2001**, *145*, 3–16; c) X. G. Sang, Q. Y. Wu, W. Q. Pang, *Mater. Chem. Phys.* **2003**, *82*, 405; d) I. Honma, S. Nomura, H. Nakajima, *J. Membr. Sci.* **2001**, *185*, 83–94; e) J.-D. Kim, I. Honma, *Solid State Ionics* **2005**, *176*, 547–552.

[3] a) Y. S. Kim, F. Wang, M. Hickner, T. A. Zawodzinski, J. E. McGrath, *J. Membr. Sci.* **2003**, *212*, 263–282; b) B. Tazi, O. Savadogo, *Electrochim. Acta* **2000**, *45*, 4329–4339; c) I. V. Kozhevnikov, *J. Mol. Catal. A* **2007**, *262*, 86; d) J. L. Malers, M. A. Sweikart, J. L. Horan, J. A. Turner, A. H. Herring, *J. Power Sources* **2007**, *172*, 83.

[4] a) V. Ramani, H. R. Kunz, J. M. Fenton, *J. Membr. Sci.* **2004**, *232*, 31–44; b) A. M. Herring, *Polym. Rev.* **2006**, *46*, 245; c) G. Inzelt, M. Pineri, J. W. Schultze, M. A. Vorotyntsev, *Electrochim. Acta* **2000**, *45*, 2403–2421; d) A. Verma, K. Scott, *J. Solid State Electrochem.* **2010**, *14*, 213–219.

[5] a) J.-D. Kim, I. Honma, *Solid State Ionics* **2005**, *176*, 547–552; b) M.-Q. Li, Z.-G. Shao, K. Scott, *J. Power Sources* **2008**, *183*, 69; c) A. Verma, K. Scott, *J. Solid State Electrochem.* **2010**, *14*, 213–219.

[6] a) M. L. Wei, C. He, W. J. Hua, C. Y. Duan, S. H. Li, Q. J. Meng, *J. Am. Chem. Soc.* **2006**, *128*, 13318–13319; b) M. L. Wei, C. He, Q. Z. Sun, Q. J. Meng, C. Y. Duan, *Inorg. Chem.* **2007**, *46*, 5957–5966; c) C. Y. Duan, M. L. Wei, D. Guo, C. He, Q. J. Meng, *J. Am. Chem. Soc.* **2010**, *132*, 3321–3330; d) M. L. Wei, H. Y. Xu, R. P. Sun, *J. Coord. Chem.* **2009**, *62*, 1989–2002.

[7] a) M. Sadakiyo, T. Yamada, H. Kitagawa, *J. Am. Chem. Soc.* **2009**, *131*, 9906–9907; b) W. A. England, M. G. Cross, A. Hamnett, P. J. Wiseman, J. B. Goodenough, *Solid State Ionics* **1980**, *1*, 231–249.

[8] a) K. D. Kreuer, S. J. Paddison, E. Spohr, M. Schuster, *Chem. Rev.* **2004**, *104*, 4637–4678; b) R. C. T. Slade, A. Hardwick, P. G. Dickens, *Solid State Ionics* **1983**, *9–10*, 1093–1098; c) G. Alberti, M. Casciola, *Solid State Ionics* **2001**, *145*, 3–16.

[9] R. Supplit, A. Sugawara, H. Peterlik, R. Kikuchi, T. Okubo, *Eur. J. Inorg. Chem.* **2010**, 3993–3999.

[10] a) M. J. Janic, R. J. Davis, M. Neurock, *J. Am. Chem. Soc.* **2005**, *127*, 5238–5245; b) E. G. Hayashi, J. B. Moffat, *J. Catal.* **1983**, *83*, 192; c) I. Honma, S. Nomura, H. Nakajima, *J. Membr. Sci.* **2001**, *185*, 83–94.

[11] K. D. Kreuer, A. Rabenau, W. Weppner, *Angew. Chem.* **1982**, *94*, 212; *Angew. Chem. Int. Ed. Engl.* **1982**, *21*, 208–209.

[12] N. Agmon, *Chem. Phys. Lett.* **1995**, *244*, 456–462.

[13] R. D. Claude, F. Michel, F. Raymonde, T. Rene, *Inorg. Chem.* **1983**, *22*, 207–216.

[14] P. G. Simapson, A. Vinciguerra, J. V. Quagliano, *Inorg. Chem.* **1963**, *2*, 282–286.

[15] Q. Y. Wu, S. L. Zhao, J. M. Wang, J. Q. Zhang, *J. Solid State Electrochem.* **2007**, *11*, 240–243.

[16] *SMART* and *SAINT*, Area Detector Control and Integration Software, Siemens Analytical X-ray Systems, Inc., Madison, WI, **1996**.

[17] G. M. Sheldrick, *SHELXTL*, v5.1, *Software Reference Manual*, Bruker AXS, Inc., Madison, WI, **1997**.

Received: October 26, 2010
Published Online: February 15, 2011

